LETTER • OPEN ACCESS

Drastic reduction of nutrient loading to a reservoir alters its resistance to impacts of extreme climatic events

To cite this article: Elias Munthali *et al* 2022 *Environ. Res. Lett.* **17** 084007

View the article online for updates and enhancements.

ENVIRONMENTAL RESEARCH
LETTERS

CrossMark

LETTER

Drastic reduction of nutrient loading to a reservoir alters its resistance to impacts of extreme climatic events

Elias Munthali[1,2,3,4,*] ![ORCID], Lisette N de Senerpont Domis[3,5] and Rafael Marcé[1,2]

1 Catalan Institute for Water Research (ICRA), Emili Grahit 101, 17003 Girona, Spain
2 University of Girona, Girona, Spain
3 Netherlands Institute of Ecology (NIOO-KNAW), Droevendaalsesteeg 10, Wageningen, 6708 PB, The Netherlands
4 Northern Region Water Board, Bloemwater Street, P/Bag 94, Mzuzu, Malawi
5 Aquatic Ecology and Water Quality Management Group, Department of Environmental Sciences, Wageningen University, Droevendaalsesteeg 3a, 6708 PB, Wageningen, The Netherlands
* Author to whom any correspondence should be addressed.

E-mail: elias.munthali@gmail.com

Abstract

By perturbing ecosystems, extreme climatic events (ECEs) can impair ecosystems' resistance and resilience to other pressures, leading to cascading effects on the continued provision of their ecosystem services. In aquatic ecology, most of the studies linking impacts of perturbations on ecosystems are based on controlled experiments and modeling, rather than real-world data. Using a 55 year dataset of hydrometeorological and reservoir water quality variables from the Ter catchment in Spain, we fill this gap by applying non-linear dynamics and extreme value theory concepts to test whether trophic state modulates reservoir ecosystem's response to ECEs. We show that both Granger causality between hydrometeorological and water quality variables and effects of ECEs on reservoir water quality diminish after drastic reduction in nutrient loading, supporting our hypothesis that the ecosystem's trophic state modulates its resistance to ECEs. Thus, by safeguarding reservoirs from nutrient pollution, water resources managers can ameliorate impacts of ECEs on ecosystem health.

1. Introduction

Eutrophication, i.e. the over enrichment of aquatic ecosystems with nutrients (Carpenter 2005), is one of the major challenges affecting the provision of aquatic ecosystem services. In its fifth global environment outlook report, the United Nations Environment Programme estimates that over 40% of the world's water bodies are experiencing moderate to heavy eutrophication (Xia *et al* 2016). Eutrophication increases drinking water treatment costs through increased organic matter from algal blooms (Foley *et al* 2012) or high iron and manganese concentrations (Munger *et al* 2019) promoted by anoxia (Carpenter 2005) and threatens water-based recreational activities from the proliferation of toxin producing cyanobacteria blooms (Padedda *et al* 2017).

Climate change might worsen eutrophication through increasing water temperature, intense or reduced precipitation, changes in wind speed and direction and solar radiation (Xia *et al* 2016). As the climate is changing, so too are the occurrence, intensity, magnitude and variability of extreme climatic events (ECEs) such as heatwaves, droughts and heavy precipitation (IPCC 2014). In ecology, ECEs are episodes where unusual values of climate variables result in responses of an ecosystem that are outside the range of normal variability (Smith 2013). By perturbing lake ecosystems, ECEs may impede the provision of aquatic ecosystem services.

The resistance and resilience of lakes to impacts of ECEs may depend more on preceding lake conditions than on characteristics of the extreme events themselves (Thayne *et al* 2021). Resistance is how (in)susceptible the system is to perturbation (Mitra *et al* 2015, Nimmo *et al* 2015), whereas ecological resilience is the extent to which a system recovers (to its original or alternative state) after a perturbation

(Perfecto *et al* 2019, Thayne *et al* 2021), or the amount of disturbance a system can withstand without flipping into another state (Folke *et al* 2004).

The degree to which ECEs impact eutrophication related processes in water bodies varies with flow rate, morphology, geographical location and season, making the generalizations of responses impractical (Delpla *et al* 2009, Mosley 2015). For instance, while high air temperatures have been reported to increase stratification, leading to eutrophication in lakes from internal nutrient loading (Collins *et al* 2019), elsewhere, stratification is reported to have reduced nutrients in surface water layers (Xia *et al* 2016). Droughts have been reported to increase eutrophication and algal blooms in mesotrophic-eutrophic lakes (Lisi and Hein 2019), due to reduced lake volumes, which concentrates nutrients and promotes cyanobacteria blooms (Wright *et al* 2014); and increased frequency of water column mixing events (Soares *et al* 2019), which promotes internal nutrient loading, hence fuelling cyanobacterial blooms. Yet, in the Mediterranean region, lower water levels are reported to have prevented cyanobacteria blooms by promoting the abundance of macrophyte that outcompeted the bloom causing cyanobacteria (Bakker and Hilt 2016). While intense rainfall has been reported to decrease algal blooms due to the reduction of light intensity through high turbidity and lake flushing (Xia *et al* 2016), in the floodplain lakes of the lower Dutch Rhine river, high rainfall intensity caused cyanobacterial blooms due to an influx of high nutrient river water through floods (Bakker and Hilt 2016). Also, floods are reported to have caused increased phytoplankton production in Gollinsee Lake due to anoxia-induced phosphorus release from the sediments (Brothers *et al* 2014). Furthermore, for shallow lakes, rising water levels inhibit light transmittance to lake bed macrophytes, leading to loss of their competitive advantage over phytoplankton and the subsequent dominance of cyanobacterial species (Bakker and Hilt 2016).

Such varied responses call for identifying modulators of lake responses to climate extremes, and we posit that lakes' trophic state might be one of the key factors.

The transient nature of most ECEs prompts researchers to rely on information, automatically collected at high frequency in lakes and rivers, to study their impacts on water quality (Marcé *et al* 2016). However, such a reliance on high frequency information is, to some extent, due to lack of appropriate methods to address these questions using low frequency (e.g. monthly) data, thereby side-lining the much more abundant long-term water quality records gathered from many aquatic ecosystems across the world. In addition, the majority of studies linking impacts of ECEs on ecosystems arise from highly controlled experiments (Veraart *et al* 2011) and modelling (Dakos *et al* 2012), hence are far

removed from real-world data (Veraart *et al* 2011). In this study, an innovative time-series approach is applied to long term monthly monitoring data, from a real-world system, to assess the role of the ecosystem's trophic state in modulating the resistance of water quality to impacts of ECEs. We took advantage of data from the long-term water quality monitoring program at Sau Reservoir (Spain) to unravel the behaviour of water quality under ECEs. During the last 55 years, Sau switched between two contrasting trophic states, following a drastic reduction in nutrient loading. We tested the hypothesis that the change in the trophic state of the reservoir significantly increased the resistance of the system's water quality to impacts of ECEs.

2. Data and methods

2.1. Study site
Sau Reservoir (41°58′N; 2°22′E, maximum depth 60 m, area 7.6 km², mean hydraulic retention time of 90 days) is located on the Ter River, in North East Spain. Its catchment area is 1790 km², with forestry (78%), arable farming (16%) and urbanization as the main land uses (López *et al* 2011). Sau Reservoir was built in 1963 for hydropower and water supply to 4 million people in the Barcelona Metropolitan area (Ordóñez *et al* 2010). Sau Reservoir lies downstream from a densely populated area where, between the years of 1991 and 1995, 16 wastewater treatment plants (WWTPs) were built, designed to treat waste water for 530 563 inhabitant-equivalents, representing 95% of the population upstream from the reservoir. The WWTPs were upgraded to secondary treatment during the early 2000s (Marcé *et al* 2006). The eutrophication process of Sau Reservoir is well described in the literature (Armengol *et al* 1986, Vidal and Om 1993, Armengol *et al* 1999, Marcé *et al* 2004, 2008b, 2010), showing an increase in nutrients loads from the 1960s to the early 1990s, accompanied by an increase in pigment concentrations and anoxia extent. From the late 1990s onwards, nutrient loads and anoxia have decreased substantially as a result of the WWTPs built upstream from the reservoir, which entailed a major reduction of organic matter and nutrient loads to the reservoir, with a sharp decrease of ammonium to nitrate molar ratio, from ∼2.5 to 0.1 (Marcé *et al* 2008b). These changes improved the trophic status of the system, which previously experienced recurrent episodes of algal blooms and extended deep water anoxia (Ordóñez *et al* 2010).

2.2. Data
This study utilized (a) daily 20 km grid interpolated rainfall (Kg m⁻² s⁻¹) and air temperature (°C) of the Escenarios-PNACC dataset (Herrera *et al* 2012, 2016) from 1950 to 2015; (b) daily observations of hydrological time series of inflows (m³ s⁻¹) and reservoir water level (m.a.s.l) and monthly reservoir water

quality records of temperature (T_w, °C), dissolved oxygen (mg DO/l), nitrate (mg NO_3^-/l), ammonium (mg NH_4^+/l) and total phosphorus (mg TP/l) from 1964 to 2019, sampled from several depths at the deepest part of the reservoir. The data was supplied by the Ens d'Abastament d'Aigua Ter-Llobregat. Further details on the water quality data are explained elsewhere in Marcé *et al* (2008b), López *et al* (2011) and Šimek *et al* (2011).

2.3. Data analysis

Hydrometeorological and reservoir water quality data were QC/QA checked and several climate indices were calculated before the main analyses were performed. First, the hydrometeorological variables were used as a set of predictors to infer causality, across quantiles, on the epilimnetic and hypolimnetic water quality variables (figure S19, stage 3), before (1963–1991) and after (1997–2015) the building and upgrading of WWTPs (hereafter referred to as before or after WWTPs). Second, climate indices of heatwaves, drought, and wet conditions were coupled to the epilimnetic and hypolimnetic timeseries to assess the behaviour of water quality during ECEs (figure S19, stage 4), before and after WWTPs.

2.3.1. Heatwave indices

Computation of heatwave indices applied the Heatwave Magnitude Index Daily (HWMID) framework (Russo *et al* 2015) by transforming the time series of daily maximum air temperature (Tmax), from Escenarios-PNACC dataset, into an index. In this framework, a heatwave is defined as a period of 3 consecutive days in which the maximum temperature is above the 90th percentile of the daily maxima in the reference period of 1981–2010, centred on a 31 day window (text S2). HWMID calculations were implemented in the 'extRemes 2.0-0' package (Gilleland and Katz 2016).

2.3.2. Drought/wetness indices

Drought and wetness indices were derived from precipitation, streamflow and reservoir water level time series, using the non-parametric Standardized Drought Analysis Toolbox (Hao and AghaKouchak 2014, Farahmand and AghaKouchak 2015) (text S1), resulting into the non-parametric standardized streamflow index (nSSFI), the non-parametric standardized water level index (nSLI), and the non-parametric standardized precipitation index (nSPI).

2.3.3. Epilimnion and hypolimnion water quality time series

To simplify the analyses, multi-depth water quality time series of T_w, DO, NO_3^-, NH_4^+, and TP were aggregated into an epilimnion and a hypolimnion time series. To achieve the aggregation, we supplied the LakeAnalyzer code (Read *et al* 2011) with a time series of water temperature and reservoir depth

profiles, from which the water temperature data was measured, for each day of the record. The code used such data to generate the top (metaT) and bottom (metaB) depths (m). The metaT is essentially the end of the epilimnion, whereas the metaB is the beginning of the hypolimnion. Thus, for water temperature and other reservoir water quality variables recorded at the same depth profiles supplied to the numerical code, the average value, on a particular day, was obtained by calculating the mean of all values at depths equal to and above metaT (for the epilimnion) and all values at depths equal to and below the metaB (for the hypolimnion). The output of this analysis was a single value of water quality variable for the epilimnion and hypolimnion for a particular day. Missing data in the monthly time series, for all water quality variables, were filled by interpolating small gaps of up to 3 months.

2.4. Statistical analyses

2.4.1. Granger-causality between hydrometeorological and reservoir water quality variables

This analysis aimed at establishing evidence of causality between the hydrometeorological and epilimnetic & hypolimnetic water quality timeseries, before and after WWTPs. The nonparametric Granger causality in quantiles method (Balcilar *et al* 2017), a non-linear variant of the Granger causality framework (Granger 2008), was applied to derive causal evidence. In the Granger framework, a causal model between two linear stationary time series X_t and Y_t is expressed as:

$$Y_t = \sum_{j=1}^{m} c_j X_{t-j} + \sum_{j-1}^{m} d_j Y_{t-j} + \eta_c \qquad (1)$$

where η_c is an uncorrelated white-noise series in the complete model. In the model, X_t is assumed to cause Y_t only if it contains information in previous terms that improves the prediction of Y_t and that information is not present in any other predictor (Granger 1988). Based on a linear autoregressive model (Silva *et al* 2021), the bivariate Granger causality arises only if the independent variable in the complete model (equation (1)) brings predictability beyond the one provided by the autocorrelation of the dependent variable at lag 1 and beyond, in the restricted model:

$$Y_t = \sum_{j-1}^{m} d_j Y_{t-j} + \eta_r \qquad (2)$$

where η_r is the uncorrelated white noise series of the restricted model.

Jeong *et al* (2012) extended the Granger framework to analysing causality in different quantiles of a time series, because other studies showed evidence of Granger-causality in tails of a variable distribution even when the mean or median did not show any evidence. They derived a 'distance measure' test statistic (J) for testing Granger causality in quantiles of

a dependent variable (Fan and Li 1999) based on the comparison of the quantiles in the prediction of Y_t with and without considering previous values of X_t.

In this study, the Jeong *et al* (2012) methodology was used to test for evidence of causality between hydrometeorological variables as predictors and epilimnetic and hypolimnetic reservoir water quality time series as response variables, using one predictor and one response variable at a time, before and after WWTPs. Granger causality was calculated at 15 discrete equidistant quantiles between 0 and 1. Significance was set at $p \sim 0.001$ for each analysis, running 1000 instances of the calculations with a random predictor, and comparing this outcome with the actual distribution of J values across quantiles (figure S2(a)). The J statistic, between the predictor and the response variable, is evaluated at 15 quantiles along the range of 0–1, and compared to the area occupied by results coming from 1000 realizations of the same calculation that uses a random predictor instead. We consider occurence of Granger causality, in a given quantile, when the J statistic calculated with the observed predictor is higher than the maximum of the 1000 values obtained with the random predictor, in the same quantile (figure S2(a)).

In order to synthesize all the information generated by this analysis (1200 quantiles tested across layers, periods, predictors, and response variables), the J statistic was aggregated over three quantile groups (low quantiles: <0.25; central quantiles: 0.25–0.75; high quantiles: >0.75). This was done by calculating the area in the J statistic plot (figure S2(b)), contained between the J statistic line of the predictor and the response variable and the maximum values of the 1000 realizations with the random predictor. Calculated over the three quantile ranges mentioned above, this procedure results in three areas, one for each quantile range (colored areas in figure S2(b)). These three areas were then normalized by dividing each area by the area under the line defined by the maximum values of the 1000 realizations obtained with the random predictors (grey area in figure S2(b)).

2.4.2. Impacts of ECEs on water quality before and after WWTPs

Impacts of ECEs on water quality were assessed by comparing median values of water quality variables in extreme and non-extreme conditions. The heatwave and drought/wetness indices (see sections 2.3.1 and 2.3.2) were used for the identification of ECEs. For the hydrometeorological events, first, nSSFI, nSLI, and nSPI index values considered beyond normal conditions (below or above zero), were clustered using the peaks-over-threshold (POT) approach (Ghil *et al* 2011), to remove autocorrelation. Then, the distribution of water quality values associated with the ECEs was split twice; first, into periods of before and after WWTPs and, second, corresponding
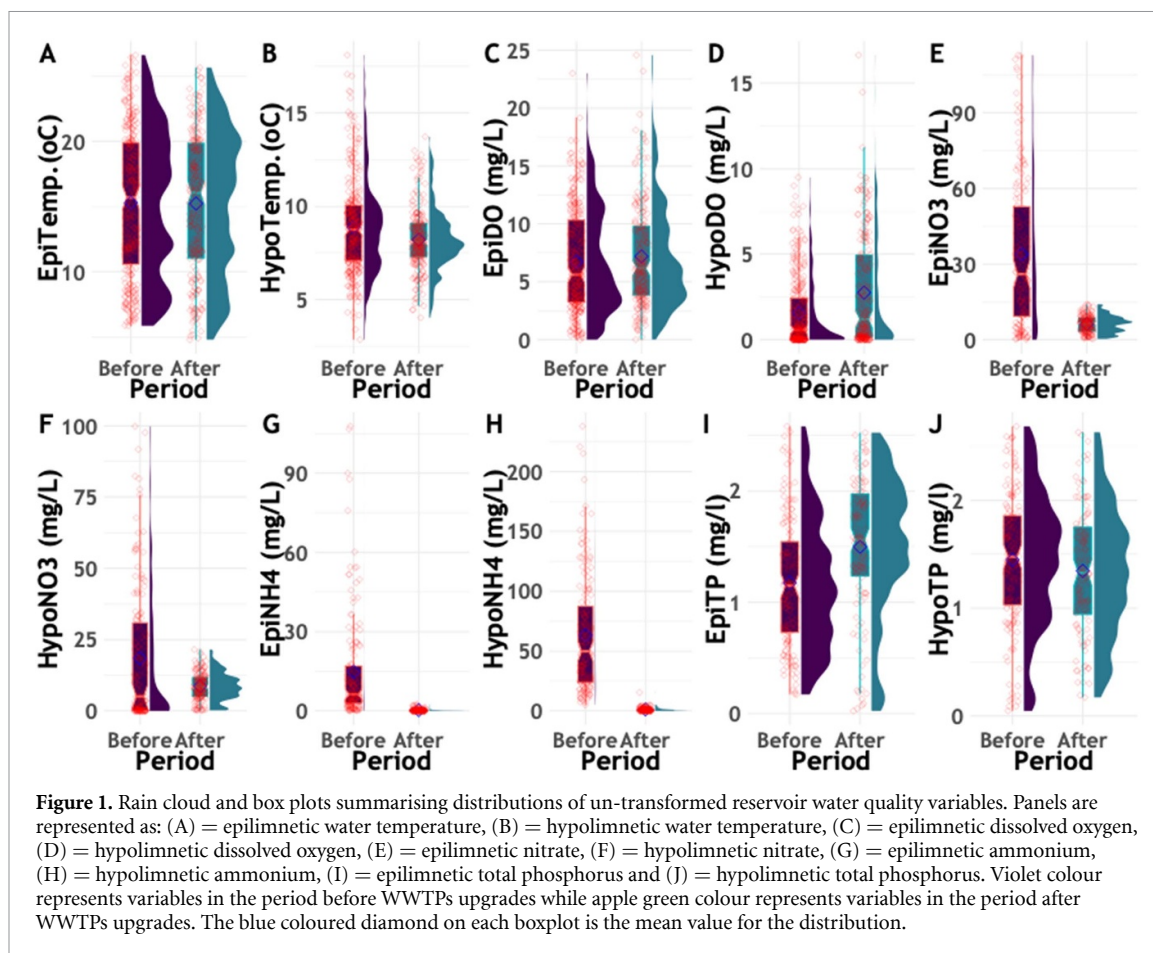
to events with indices beyond the threshold that could be considered extreme (<-1.3 & $>+1.3$) and the rest that could be considered beyond normal but not extreme ($>-1.3 <0$ & $>0 < 1.3$). Thereafter, the value of the water quality variables in the epilimnion and hypolimnion, for each event, was calculated as the median of all data corresponding to that type of event. POT analysis was performed using the POT package, version 1.1-7 (Ribatet 2011). The medians of water quality variables, in extreme and non-extreme events, for each period, were compared using the Welch's test (Zheng *et al* 2013) on ranked values, which allows a robust comparison of non-normal distributions with different sample sizes and variances. The results of the Welch's test were reported as p-values, that were supplemented by the Hedges's g_s effect size metric (Lakens 2013). Hedges's g_s is a bias corrected standardized median difference (Cohen's d_s) measuring the degree to which sample results depart from anticipations expressed in the null hypothesis being tested from the data (Thompson 2007). The following Hedges's g_s thresholds for stating effect sizes were adopted: small ($g_s = 0.2$); medium ($g_s = 0.5$) and large ($g_s = 0.8$) (Thompson 2007, Lakens 2013). For heatwaves, the low number of events and their accumulation exclusively in summer months (June–August), required a different approach. A summer was considered to experience a heatwave if the HWMID value exceeded zero on any day during that summer. Thus, a maximum of one heatwave event could be defined for each year. Subsequently, every summer was assigned with values for the water quality variables. Assuming that a heatwave would have a long-lasting imprint on water quality during the summer period, the value of water quality variable in August was assigned. Thus, each summer either had or did not have a heatwave, and was paired with epilimnetic and hypolimnetic water quality data in August, after which, the analyses proceeded in the same way as the analyses examining the impacts of extreme drought and wet events.

All calculations and graphical illustrations were implemented in (R Core Team 2017).

3. Results

3.1. Historical changes in hydrometeorological and water quality variables

The period after WWTPs was characterized by lower medians of precipitation and inflow (Mann Whitney tests on pre-whitened series) than before WWTPs (figure S16, table S1). Interestingly, the frequency of extreme droughts, relative to total drought events, increased after WWTPs, from 5%–10% to 15%–16%, depending on the index (table S3(a)). Summers with heat waves also increased from 35% to 58% after WWTPs (table S3(c)). In contrast, the frequency of extreme wet events decreased after WWTPs,

Figure 1. Rain cloud and box plots summarising distributions of un-transformed reservoir water quality variables. Panels are represented as: (A) = epilimnetic water temperature, (B) = hypolimnetic water temperature, (C) = epilimnetic dissolved oxygen, (D) = hypolimnetic dissolved oxygen, (E) = epilimnetic nitrate, (F) = hypolimnetic nitrate, (G) = epilimnetic ammonium, (H) = hypolimnetic ammonium, (I) = epilimnetic total phosphorus and (J) = hypolimnetic total phosphorus. Violet colour represents variables in the period before WWTPs upgrades while apple green colour represents variables in the period after WWTPs upgrades. The blue coloured diamond on each boxplot is the mean value for the distribution.

from 9%–10% to 4%–5%, depending on the index (table S3(b)). Before WWTPs, the median of hypolimnetic DO was 105% lower than its corresponding median after WWTPs. On the other hand, the median of NH_4^+ was 98% higher than its corresponding median after WWTPs. Medians of NO_3^-, TP and T_w were statisticslly similar between the two periods (figure 1, table S2). In the epilimnion, the medians of NO_3^- and NH_4^+ were 75% and 98%, respectively, lower while the median of TP was 35% higher after WWTPs, compared with their respective medians before WWTPs (figure 1, table S2). Overall, the building and upgrading of WWTPs drastically reduced concentrations of nitrogen compounds in the reservoir, enhanced dissolved oxygen in the hypolimnetic water layers but did not seem to affect total phosphorus.

3.2. Causal relationships between hydrometeorological drivers and water quality variables

The building and upgrading of WWTPs affected the strength of Granger causality between hydrometeorology and water quality variables (figure 2, supplementary figures S3 and S4). The causal influence of inflow on hypolimnetic DO was particularly strong before WWTPs but disappeared after WWTPs

(figures 2 and S3). In contrast, Granger causality of inflow on DO was altogether absent in the epilimnion in both periods (figures 2 and S4). After WWTPs, hypolimnetic NO_3^- showed causality with Tmax, covering the whole quantile range, and low to mid quantiles for epilimnetic NO_3^- and DO (figures 2, S3 and S4). TP was unresponsive to the four predictors, in both periods, except for a weak Granger causality with Tmax before WWTPs (figures 2 and S3). Unsurprisingly, Tmax showed a strong causality with T_w, which became even stronger in the epilimnion after WWTPs (figures 2, S3 and S4).

3.3. Impact of ECEs on water quality before and after WWTPs

Overall, the hypolimnion manifested a clear reduction of the impacts of ECEs after WWTPs, whereas the response in the epilimnion defied simple description and suggested a complex set of responses both before and after WWTPs (figure 3, tables S4–S8).

In the hypolimnion, extreme (streamflow) droughts were associated with a lower median of DO (moderate Hedges's g_s, figures 3 and S5, panel (C)) and higher medians for NH_4^+ (moderate Hedges's g_s, figures 3 and S7, panel (C)) and T_w (weak Hedges's g_s, figures 3 and S9, panel (C)) relative to non-extreme drought conditions, before WWTPs. However, after
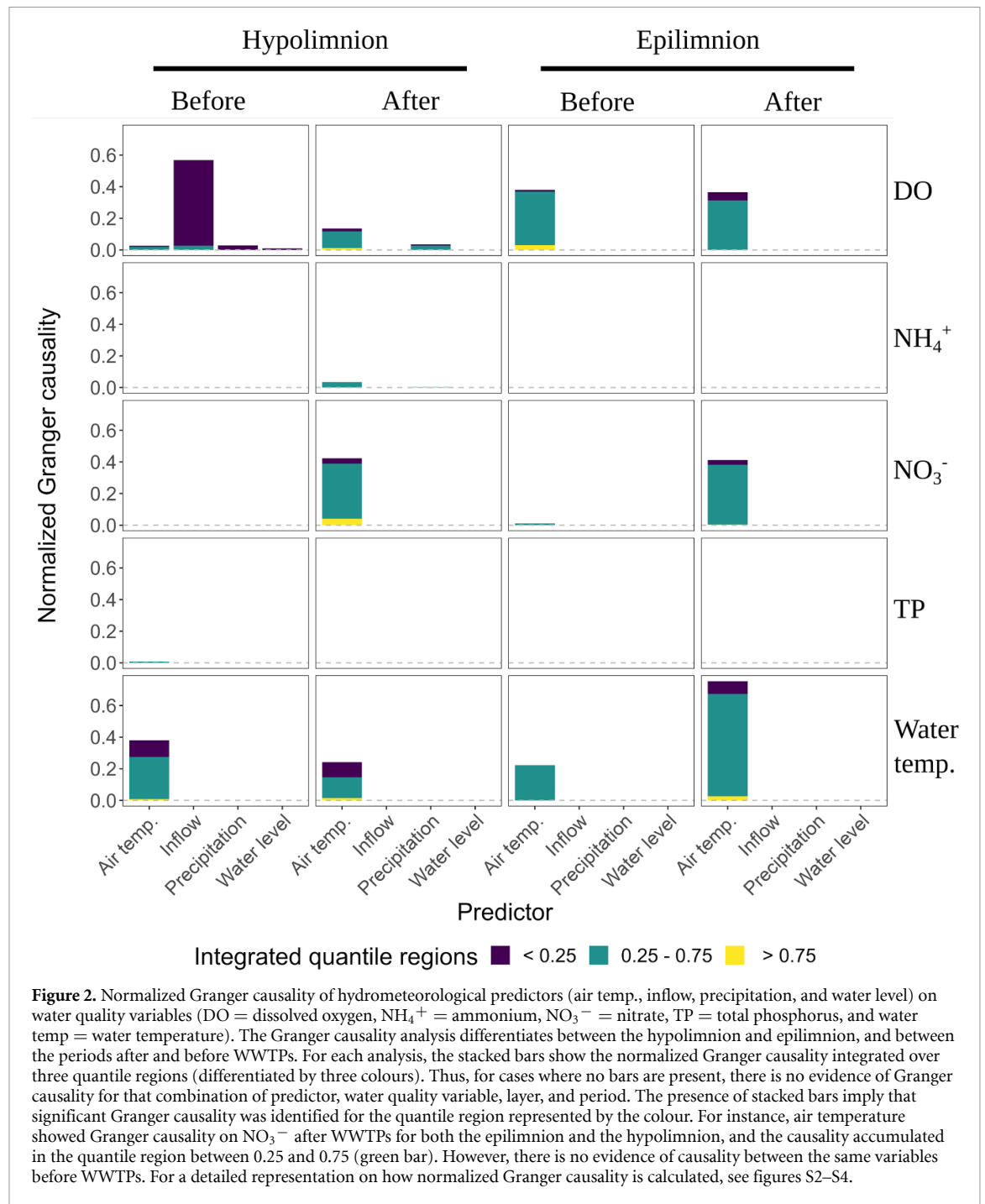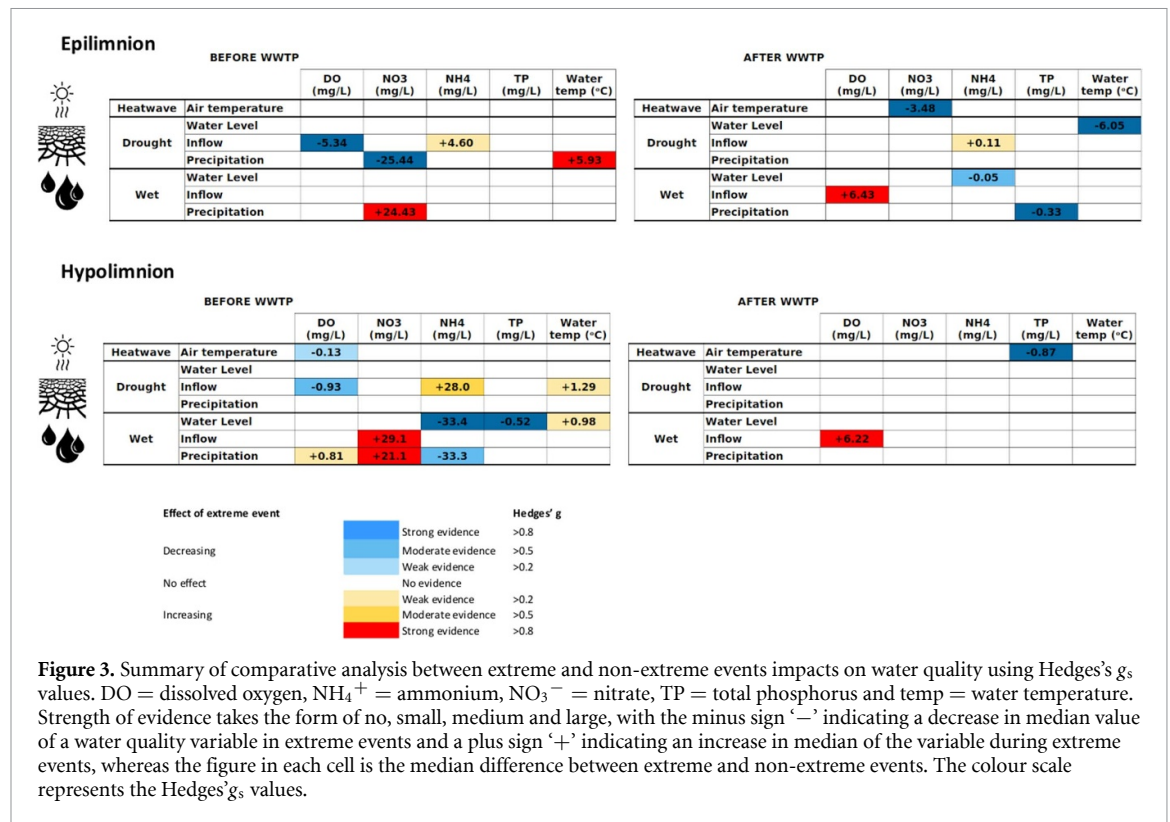
Figure 2. Normalized Granger causality of hydrometeorological predictors (air temp., inflow, precipitation, and water level) on water quality variables (DO = dissolved oxygen, NH_4^+ = ammonium, NO_3^- = nitrate, TP = total phosphorus, and water temp = water temperature). The Granger causality analysis differentiates between the hypolimnion and epilimnion, and between the periods after and before WWTPs. For each analysis, the stacked bars show the normalized Granger causality integrated over three quantile regions (differentiated by three colours). Thus, for cases where no bars are present, there is no evidence of Granger causality for that combination of predictor, water quality variable, layer, and period. The presence of stacked bars imply that significant Granger causality was identified for the quantile region represented by the colour. For instance, air temperature showed Granger causality on NO_3^- after WWTPs for both the epilimnion and the hypolimnion, and the causality accumulated in the quantile region between 0.25 and 0.75 (green bar). However, there is no evidence of causality between the same variables before WWTPs. For a detailed representation on how normalized Granger causality is calculated, see figures S2–S4.

WWTPs, none of the extreme drought conditions was associated with changes in any water quality variable. Extreme (inflow, water level & precipitation) wet events were associated with higher medians of DO (weak Hedges's g_s, figures 3 and S5, panel (M)), NO_3^- (strong Hedges's g_s, figures 3 and S6, panels (E), (M)) and T_w (weak Hedges's g_s, figures 3 and S9, panel (I)) and lower medians of NH_4^+ (strong & moderate Hedges's g_s, figures 3 and S7, panels (I), (M)) and TP (strong Hedges's g_s, figure 3 and table S7), relative to their respective non-extreme wet conditions, before WWTPs. While similar (streamflow) events were associated with a higher median value of DO (strong Hedges's g_s, figures 3 and S5, panel (F)),

the rest of water quality variables, however, were unaffected by extreme wet conditions after WWTPs. Before WWTPs, summers with heatwaves were associated with a lower median of DO (weak Hedges's g_s, figures 3 and S5, panel (A)) compared to summers without heatwaves, whereas the rest of the water quality variables were unresponsive to heatwaves. After WWTPs, summers with heatwaves were associated with a lower median of TP (strong Hedges's g_s, figure 3 and table S7) compared to summers without heatwaves, whereas no other water quality variable responded to heatwaves (figure 3, tables S4–S8).

In the epilimnion, extreme (inflow & precipitation) drought events were associated with lower

Epilimnion

BEFORE WWTP

		DO (mg/L)	NO3 (mg/L)	NH4 (mg/L)	TP (mg/L)	Water temp (°C)
Heatwave	Air temperature					
Drought	Water Level					
	Inflow	-5.34		+4.60		
	Precipitation		-25.44			+5.93
Wet	Water Level					
	Inflow					
	Precipitation		+24.43			

AFTER WWTP

		DO (mg/L)	NO3 (mg/L)	NH4 (mg/L)	TP (mg/L)	Water temp (°C)
Heatwave	Air temperature		-3.48			
Drought	Water Level					-6.05
	Inflow			+0.11		
	Precipitation					
Wet	Water Level			-0.05		
	Inflow		+6.43			
	Precipitation				-0.33	

Hypolimnion

BEFORE WWTP

		DO (mg/L)	NO3 (mg/L)	NH4 (mg/L)	TP (mg/L)	Water temp (°C)
Heatwave	Air temperature	-0.13				
Drought	Water Level					
	Inflow	-0.93		+28.0		+1.29
	Precipitation					
Wet	Water Level			-33.4	-0.52	+0.98
	Inflow		+29.1			
	Precipitation	+0.81	+21.1	-33.3		

AFTER WWTP

		DO (mg/L)	NO3 (mg/L)	NH4 (mg/L)	TP (mg/L)	Water temp (°C)
Heatwave	Air temperature				-0.87	
Drought	Water Level					
	Inflow					
	Precipitation					
Wet	Water Level					
	Inflow	+6.22				
	Precipitation					

Effect of extreme event		Hedges' g
Decreasing	Strong evidence	>0.8
	Moderate evidence	>0.5
	Weak evidence	>0.2
No effect	No evidence	
	Weak evidence	>0.2
Increasing	Moderate evidence	>0.5
	Strong evidence	>0.8

Figure 3. Summary of comparative analysis between extreme and non-extreme events impacts on water quality using Hedges's g_s values. DO = dissolved oxygen, NH_4^+ = ammonium, NO_3^- = nitrate, TP = total phosphorus and temp = water temperature. Strength of evidence takes the form of no, small, medium and large, with the minus sign '−' indicating a decrease in median value of a water quality variable in extreme events and a plus sign '+' indicating an increase in median of the variable during extreme events, whereas the figure in each cell is the median difference between extreme and non-extreme events. The colour scale represents the Hedges's g_s values.

medians of DO (strong Hedges's g_s, figures 3 and S10, panel (C)) and NO_3^- (strong Hedges's g_s, figures 3 and S11, panel (K)) and higher medians of NH_4^+ (weak Hedges's g_s figures 3 and S12, panel (C)) and T_w (strong Hedges's g_s figures 3 and S14, panel (K)), relative to their respective non-extreme drought conditions, before WWTPs. Similar extreme (inflow & water level) droughts were not associated with any changes in DO but corresponded to a higher median of NH_4^+ (weak Hedges's g_s, figures 3 and S12, panel (D)) and a lower median of T_w (strong Hedges's g_s figure 3 and table S8) after WWTPs. Extreme (precipitation) wet events were associated with a higher median of NO_3^- (strong Hedges's g_s, figures 3 and S11, panel (M)) relative to their non-extreme conditions before WWTPs. Similar extreme (precipitation) wet events were not associated with any change in NO_3^- but corresponded to a lower median of TP (strong Hedges's g_s, figure 3 and table S7), after WWTPs. Furthermore, extreme (water level and inflow) wet conditions were associated with a lower median of NH_4^+ (weak Hedges's g_s figure 3 and table S6) and a higher median value of DO (strong Hedges's g_s, figures 3 and S10, panel (F)), respectively, after WWTPs. Summers with heat waves were associated with a decrease in the median of NO_3^- (strong Hedges's g_s, figures 3 and S11, panel (B)) relative to summers without heat waves after WWTPs, whereas no heat wave effect was observed on any water quality variable before WWTPs (tables S4–S8). After WWTPs, summers with heatwaves were associated with a lower median of TP (strong Hedges's g_s,

figure 3 and table S7) compared to summers without heatwaves, whereas no any other water quality variable responded to heatwaves (figure 3, tables S4–S8).

4. Discussion

The hypothesis that a change in trophic state of the reservoir increased resistance of the system's water quality to impacts of ECEs, was supported by results from both the Granger causality in quantile (particularly on DO) and behaviour of water quality under ECEs analyses. Both analyses also suggested that the change in resistance of water quality to ECEs, before and after WWTPs, was particularly prominent in the hypolimnion, whereas the epilimnion retained a comparable sensitivity to ECEs. The absence of statistically significant differences in medians of almost all water quality variables (except for DO), between extreme and non-extreme hydrological events, in the hypolimnion, i.e. the absence of impacts of hydrological extreme events on water quality, after WWTPs, is interpreted as increased resistance, following the definitions provided for by Perfecto *et al* (2019), Thayne *et al* (2021) and Mitra *et al* (2015). Conversely, in the epilimnion, the presence of statistically significant differences in medians of water quality variables between extreme and non-extreme hydrological events, in both periods, implies the retention of sensitivity to impacts of those ECEs, hence interpreted as lack of or less resistance. The increased resistance of water quality to ECEs in the hypolimnion, after WWTPs, coincided with an

increased frequency of extreme droughts and heat-waves, making it unlikely that these observations were an artefact caused by a reduction in the number of ECEs.

The differences in behaviour between the epilimnion and hypolimnion suggest that reservoir biogeochemical processes play a fundamental role in defining the response of water quality to ECEs. We postulate that the observed differences in Granger causality and impacts of ECEs on DO concentrations are governed by (a) differing metabolic pathways of anabolism and catabolism dominating the epilimnion and hypolimnion respectively, and (b) stronger water-air coupling in the epilimnion making it susceptible to transient hydrometeorological conditions. The dominance of primary production in the epilimnion may have influenced the observed lack of causality between hydrometeorological variables and water quality (except Tmax). Phytoplankton is a dynamic component of lake ecosystems, with a generation time in the order of days, whereas the monitoring program in Sau Reservoir was on a monthly basis. While a monthly sampling resolution can capture changes driven by eutrophication (Pomati *et al* 2012, Jochimsen *et al* 2013), it is insufficient to capture the short term dynamics of primary producers, operating on time scales of hours to days. Using monthly data may have limited the capability to predict water quality changes in the epilimnion.

Hypolimnetic water quality was more sensitive to ECEs probably due to the crucial role of organic matter degradation as a pathway for energy and matter flow in deep layers. Organic matter degradation in the hypolimnion is driven by the flow of organic materials from the river and the epilimnion, and the availability of electron acceptors (DO and NO_3^-). Degradation of organic matter does not show short-term oscillations typical of primary production processes (Bastviken *et al* 2004), which may explain our observed causality between inflow and DO.

High causality and the significant impacts of ECEs found in the hypolimnion, before WWTPs, could also be explained by background water quality conditions. Before the operationalization of the WWTPs, the hypolimnion was anoxic, with a very high NH_4^+ to NO_3^- molar ratio (Marcé *et al* 2008b). This scenario suggests a stronger role of organic matter degradation processes that keeps DO levels low. The high NH_4^+ to NO_3^- ratio originated from the fact that most dissolved nitrogen entered the reservoir as NH_4^+ and the presence of anoxia promoted denitrification (Hedin *et al* 1998, Burgin *et al* 2011). Thus, extreme drought conditions would exacerbate respiration processes, hence decreasing DO and increasing NH_4^+ concentrations. In contrast, extreme wet conditions would favour re-oxygenation, increase the NO_3^- load from non-point sources, and dilute NH_4^+ concentrations

from WWTPs. After WWTPs, only re-oxygenation during extreme wet events remained, suggesting a reduced role of respiration processes in the hypolimnion, which was no longer responding to extreme droughts through low DO and high NH_4^+ levels. Thus, the dramatic decrease in NH_4^+ concentration blurred the dilution effect of extreme wet events.

5. Conclusion

This study provides a novel approach to infer causality between hydrometeorological extreme events and reservoir water quality using low-frequency water quality time-series. The non-parametric causality-in-quantile approach to analysing a long term, low frequency dataset, gathered from a real and complex system, shows that trophic state modulates the resistance of reservoir water quality variables to effects of ECEs and that the deeper water layers are more strongly impacted by these events and hence their resistance is more dependent on trophic state. We hypothesise that by keeping reservoirs in good trophic state (mesotrophic to oligotrophic), their water quality becomes more resistant to impacts of extreme events, giving water resources managers some control in dealing with adverse effects of the climate extremes. We conclude that besides improving water quality (in order to achieve UN Sustainable Development Goal 6.3), having water uncompromised by nutrient pollution also ameliorates adverse effects of climate extremes on reservoir water quality.

Data availability statement

The data that support the findings of this study are available upon reasonable request from the authors.

ORCID iD

Elias Munthali ● https://orcid.org/0000-0001-6681-4371

References

Armengol J *et al* 1986 Phosphorus budgets and forms of phosphorus in the Sau reservoir sediment: an interpretation of the limnological record *Hydrobiologia* **143** 331–6

Armengol J *et al* 1999 Longitudinal processes in canyon type reservoirs: the case of sau (N E Spain) eds J G Tundisi and M Straskraba *Theoretical Reservoir Ecology and Its Applications* (Rio de Janeiro: International Institute of Ecology, Brazilian Academy of Sciences and Backhuys Publishers) pp 313–45

Bakker E S and Hilt S 2016 Impact of water-level fluctuations on cyanobacterial blooms: options for management *Aquat. Ecol.* **50** 485–98

Balcilar M, Bekiros S and Gupta R 2017 The role of news-based uncertainty indices in predicting oil markets: a hybrid nonparametric quantile causality method *Empir. Econ.* **53** 879–89

Bastviken D *et al* 2004 Degradation of dissolved organic matter in oxic and anoxic lake water *Limnol. Oceanogr.* **49** 109–16

Brothers S *et al* 2014 A feedback loop links brownification and anoxia in a temperate, shallow lake *Limnol. Oceanogr.* **59** 1388–98

Burgin A J *et al* 2011 Beyond carbon and nitrogen: how the microbial energy economy couples elemental cycles in diverse ecosystems *Front. Ecol. Environ.* **9** 44–52

Carpenter S R 2005 Eutrophication of aquatic ecosystems: bistability and soil phosphorus *Proc. Natl Acad. Sci.* **102** 10002–5

Collins S M *et al* 2019 Winter precipitation and summer temperature predict lake water quality at macroscales *Water Resour. Res.* **55** 2708–21

Dakos V *et al* 2012 Methods for detecting early warnings of critical transitions in time series illustrated using simulated ecological data *PLoS One* **7** e41010

Delpla I *et al* 2009 Impacts of climate change on surface water quality in relation to drinking water production *Environ. Int.* **35** 1225–33

Fan Y and Li Q 1999 Central limit theorem for degenerate U-statistics of absolutely regular processes with applications to model specification testing *J. Nonparametr. Stat.* **10** 245–71

Farahmand A and AghaKouchak A 2015 A generalized framework for deriving nonparametric standardized drought indicators *Adv. Water Resour.* **76** 140–5

Foley B *et al* 2012 Long-term changes in oxygen depletion in a small temperate lake: effects of climate change and eutrophication: oxygen depletion in a small lake *Freshw. Biol.* **57** 278–89

Folke C *et al* 2004 Regime shifts, resilience, and biodiversity in ecosystem management *Annu. Rev. Ecol. Evol. Syst.* **35** 557–81

Ghil M *et al* 2011 Extreme events: dynamics, statistics and prediction *Nonlinear Process. Geophys.* **18** 295–350

Gilleland E and Katz R W 2016 extRemes 2.0: an extreme value analysis package in R *J. Stat. Softw.* **72**

Granger C W J 1988 Some recent development in a concept of causality *J. Econom.* **39** 199–211

Granger C W J 2008 Investigating causal relations by econometric models and cross-spectral methods *Econometrica* **37** 424–38

Hao Z and AghaKouchak A 2014 A nonparametric multivariate multi-index drought monitoring framework *J. Hydrometeorol.* **15** 89–101

Hedin L O *et al* 1998 Thermodynamic constraints on nitrogen transformations and other biogeochemical processes at soil-stream interfaces *Ecology* **79** 684–703

Herrera S *et al* 2012 Development and analysis of a 50-year high-resolution daily gridded precipitation dataset over Spain (Spain02): development and analysis of a 50-YEAR High-Resolution Daily Gridded Precipitation Dataset *Int. J. Climatol.* **32** 74–85

Herrera S, Fernández J and Gutiérrez J M 2016 Update of the Spain02 gridded observational dataset for EURO-CORDEX evaluation: assessing the effect of the interpolation methodology: EURO-CORDEX compliant update of Spain02 *Int. J. Climatol.* **36** 900–8

IPCC 2014 Climate change 2014 part A: global and sectoral aspects *Climate Change 2014: Impacts, Adaptation, and Vulnerability. Part A: Global and Sectoral Aspects. Contribution of Working Group II to the Fifth Assessment Report of the Intergovernmental Panel on Climate Change* ed C B Field *et al* (New York: Cambridge University Press) p 1132 (available at: papers2://publication/uuid/B8BF5043-C873-4AFD-97F9-A630782E590D)

Jeong K, Härdle W K and Song S 2012 A consistent nonparametric test for causality in quantile *Econ. Theory* **28** 861–87

Jochimsen M C, Kümmerlin R and Straile D 2013 Compensatory dynamics and the stability of phytoplankton biomass during four decades of eutrophication and oligotrophication *Ecol. Lett.* **16** 81–89

Lakens D 2013 Calculating and reporting effect sizes to facilitate cumulative science: a practical primer for t-tests and ANOVAs *Front. Psychol.* **4**

Lisi P J and Hein C L 2019 Eutrophication drives divergent water clarity responses to decadal variation in lake level *Limnol. Oceanogr.* **64** S49–59

López P, Marcé R and Armengol J 2011 Net heterotrophy and CO_2 evasion from a productive calcareous reservoir: adding complexity to the metabolism-CO_2 evasion issue *J. Geophys. Res.* **116** 1–14

Marcé R *et al* 2006 Nutrient fluxes through boundaries in the hypolimnion of Sau reservoir: Expected patterns and unanticipated processes *Limnetica* **25** 527–40

Marcé R *et al* 2008a The role of allochthonous inputs of dissolved organic carbon on the hypolimnetic oxygen content of reservoirs *Ecosystems* **11** 1035–53

Marcé R *et al* 2016 Automatic high frequency monitoring for improved lake and reservoir management *Environ. Sci. Technol.* **50** 10780–94

Marcé R, Comerma M, García J C and Armengol J 2004 A neuro-fuzzy modeling tool to estimate fluvial nutrient loads in watersheds under time-varying human impact *Limnol. Oceanogr.* **2–11** 342–55

Marcé R, Moreno-Ostos E and Armengol J 2008b The role of river inputs on the hypolimnetic chemistry of a productive reservoir: implications for management of anoxia and total phosphorus internal loading *Lake Reserv. Manage.* **24** 87–98

Marcé R, Rodríguez-Arias M A, García J C and Armengol J 2010 El Niño Southern Oscillation and climate trends impact reservoir water quality *Glob. Change Biol.* **16** 2857–65

Mitra C, Kurths J and Donner R V 2015 An integrative quantifier of multistability in complex systems based on ecological resilience *Sci. Rep.* **5** 16196

Mosley L M 2015 Drought impacts on the water quality of freshwater systems; review and integration *Earth Sci. Rev.* **140** 203–14

Munger Z W *et al* 2019 Oxygenation and hydrologic controls on iron and manganese mass budgets in a drinking-water reservoir *Lake Reserv. Manage.* **35** 277–91

Nimmo D G *et al* 2015 Vive la résistance: reviving resistance for 21st century conservation *Trends Ecol. Evol.* **30** 516–23

Ordóñez J *et al* 2010 On non-Eltonian methods of hunting Cladocera, or impacts of the introduction of planktivorous fish on zooplankton composition and clear-water phase occurrence in a Mediterranean reservoir *Hydrobiologia* **653** 119–29

Padedda B M *et al* 2017 Consequences of eutrophication in the management of water resources in Mediterranean reservoirs: a case study of Lake Cedrino (Sardinia, Italy) *Glob. Ecol. Conserv.* **12** 21–35

Perfecto I *et al* 2019 Response of coffee farms to hurricane maria: resistance and resilience from an extreme climatic event *Sci. Rep.* **9** 15668

Pomati F *et al* 2012 Effects of re-oligotrophication and climate warming on plankton richness and community stability in a deep mesotrophic lake *Oikos* **121** 1317–27

R Core Team 2017 R: a language and environment for statistical computing (available at: www.r-project.org/)

Read J S *et al* 2011 Derivation of lake mixing and stratification indices from high-resolution lake buoy data *Environ. Model. Softw.* **26** 1325–36

Ribatet M 2011 A user's guide to the pot package (version 1. 4) an introduction to the EVT the univariate case pp 1–31

Russo S, Sillmann J and Fischer E M 2015 Top ten European heatwaves since 1950 and their occurrence in the coming decades *Environ. Res. Lett.* **10** 124003

Silva F N *et al* 2021 Detecting climate teleconnections with granger causality *Geophys. Res. Lett.* **48**

Šimek K *et al* 2011 The effect of river water circulation on the distribution and functioning of reservoir microbial communities as determined by a relative distance approach *Ecosystems* **14** 1–14

Smith M D 2013 Extreme climatic events *Climate Vulnerability: Understanding and Addressing Threats to Essential Resources* vol 4 (Cambridge, MA: Academic Press) pp 71–80

Soares L M V *et al* 2019 Modelling drought impacts on the hydrodynamics of a tropical water supply reservoir *Inland Waters* **9** 422–37

Thayne M W *et al* 2021 Antecedent lake conditions shape resistance and resilience of a shallow lake ecosystem following extreme wind storms *Limnol. Oceanogr.* **67** 1–20

Thompson B 2007 Effect sizes, confidence intervals, and confidence intervals for effect sizes *Psychol. Sch.* **44** 423–32

Veraart A J *et al* 2011 Recovery rates reflect distance to a tipping point in a living system *Nature* **481** 357–9

Vidal A and Om J 1993 The eutrophication process in Sau Reservoir (NE Spain): a long term study *Int. Ver. Theor. Angew. Limnol.* **25** 1247–56

Wright B *et al* 2014 Managing water quality impacts from drought on drinking water supplies *J. Water Supply: Res. Technol. AQUA* **63** 179–88

Xia R *et al* 2016 The potential impacts of climate change factors on freshwater eutrophication: implications for research and countermeasures of water management in China *Sustainability* **8**

Zheng L, Diamond J M and Denton D L 2013 Evaluation of whole effluent toxicity data characteristics and use of Welch's T-test in the test of significant toxicity analysis *Environ. Toxicol. Chem.* **32** 468–74